Friction drive for ultra-precision machine tools: interface compliance-based model

B.N. Damazo[1], A.E. Gee[2] and A.H. Slocum[3]

[1] *Automated Production Div., National Institute of Standards and Technology, Gaithersburg, MD 20899, USA*

[2] *School of Industrial and Manufacturing Science, Cranfield University, Cranfield, Bedford, MK43 0AL, UK*

[3] *Department of Mechanical Engineering, Massachusetts Institute of Technology, Cambridge, MA 02139, USA*

Abstract

The roller/bar friction-drive is an example of a high-precision rectilinear actuator. The roller/bar friction drive offers control advantages of low backlash and dead-band due to elastic averaging within the Hertzian contact region. It also offers simplicity, both of initial design and extensibility to longer ranges (as high as of the order of meters) while incurring only marginal effort/cost in design and implementation. Furthermore, the roller/bar friction drive has not been employed extensively, this is probably due to uncertainty over issues of limitations on drive-force, transmission-gain and topology and cleanliness of the drive-bar/interface.

To address uncertainties involved in the characteristics of such a drive, analysis was undertaken with the objective of providing design-tools for a new generation of machine tools. A model was developed to predict the behavior of the contact interface using Hertzian contact stress theory.

Other goals of the study included methodologies for determining static and dynamic stiffness as a function of load and input dynamics as represented by the drive-force frequency. The model is described and comparisons with experimental results are made.

1 Precision motions: historical progress

Terms such as 'Precision' and 'Ultra-precision' are to a certain extent adaptive, taking account of the expected contemporary norms and improvements as time progresses and general levels of performance improve and deviation from spatial specifications decrease. The results of such progress are manifest in improvements in consumer artifacts such as automobile engines/superchargers, in the longevity of refrigerator compressors and the manufacture of high-volume molded precision items such as the optics for compact disc technology. Reviews of such progress have been undertaken by Taniguchi (1983) and by McKeown (1986).

For the purpose of this paper, whereas 'precision' might apply to the best machine-shop capabilities such as found in the jig-borer, 'ultra-precision' is taken to imply processes capable of repeatabilities of the order of parts in 10^6 and/or resolutions to sub-micrometer levels. These requirements bear significantly upon the specifications of actuators required to produce motion.

Particularly high performances in rectilinear actuators have been achieved using the leadscrew. An exacting requirement arose in the ruling of spectroscopic diffraction-gratings where successive groove-placement over 250 mm must be to within a fraction of a micrometer of the 'correct' position

Transactions on Engineering Sciences vol 16, © 1997 WIT Press, www.witpress.com, ISSN 1743-3533

(as defined by the median of the grooves already ruled). Having pioneered the use of interferometry for metrological applications, Michelson (1915) applied this to calibrating/correcting the repeatable errors in leadscrews for ruling-engines and, when the state of electronics permitted, Harrison at MIT implemented this as a continuous servo-correction on a machine derived from Michelson's work (Harrison and Stroke 1955). Basing two further machines on the jig-borer/measuring machines of the Moore Special Tool Co., Harrison went on to extend the size of ruled gratings to 600 mm (Harrison 1972). This interaction of the grating-ruling research community with machine-tool builders led to the employment of interferometric control on single-point lathes and other machine-tools designed for the direct manufacture of metal optical surfaces such as aspheric mirrors, to the same order of sub-wave length form tolerances and nanometric finishes (Moore 1970). Where periodic errors are deleterious, as in gratings (causing spurious 'ghost' peaks in the observed spectrum), the random error obtained with a stepper might be more tolerable. After initial work on grating engines (Gee 1982), the stepper approach was used for motion-generation in wafer step-cameras in microelelctronic VLSI circuit production.

Traditionally, the machine-tool industry has employed precision rectilinear motions to ranges covering the lengths of the required artifacts. The turning of long-cylinders and screws and the machining of long surfaces on mills, shapers and planers are examples of artifacts/processes requiring such motions and the usual actuator employed has been the precision leadscrew.

Leadscrews with micrometer capability can be obtained in lengths of more than one meter (Moore 1970). The leadscrew's merits are its intrinsic ability to 'measure' to fine accuracy over long ranges from the count of turns and the angular fraction of any part-turn. However, once a separate measurement transducer is added (e.g. an incremental scale or laser interferometer), the requirement devolves into providing smooth repeatable motion. The leadscrew continues to be used even in recent applications such as X-Y positioning in wafer-step cameras for the microelectronics industry.

An alternative drive, whose philosophy and physical lay-out has commonality with the friction drive, is the linear electric motor. Essentially, the rotor and stator of a conventional rotating motor are arranged to be rectilinear elements. Straddling a long 'rail' element, the linear electric motor has a small drive unit which can be mounted directly and integrally with the driven carriage, thereby eliminating couplings and potential error sources due to backlash and bearings. Because it is a force actuator, there are few limitations to ultimate position-resolution (Chitayat 1987) and tests have shown positioning accuracy to within 0.1μm (May-Miller, 1987).

Where the attributes of a short-range actuator are required in combination with long-range, combination of two actuators in the form of a 'hybrid' is a possibility, requiring appropriate mixed and interactive control arrangements (Sakuta 1990).

2 REQUISITES FOR HIGH PRECISION MOTION

A number of desirable characteristics may be identified for motion actuators:

(i) high static stiffness;
(ii) high dynamic stiffness;
(iii) low friction;
(iv) linearity;
(v) high intrinsic gain.

Mechanisms like the leadscrew satisfy the first characteristic and, with effort, can be made to satisfactorily yield the second. However, for low

friction, mating parts are required to be held in conditions of light interface forces, which tend to manifest lost motions on reversal such as hysteresis of which 'backlash' is a prime example. A metrology frame may be employed to compensate for such non-linearities. A further result of low absolute values of friction is the tendency of sliding surface interfaces to manifest 'sticktion', or stick-slip, an effect which is extremely deleterious to precision positioning and which is traceable to the friction associated with starting being higher than that required for sustaining motion. In combination with elasticity, imprecise skipping motion may arise at low (slow) levels of motion and/or commencement of motion following reversal. The combination of backlash and stick-slip is particularly problematical where the actuator is employed in a high-gain feedback control loop, as is often the case. When analyzed harmonically, the effective 'delay' acts as a phase-shift with considerable reduction in feedback-control stability (i.e. reduced damping and/or the tendency to oscillate spontaneously).

3 FRICTION-DRIVES: DESCRIPTION

The friction-drive (also known as the 'capstan' drive) is a straightforward concept. Rectilinear drive motion/force is generated by rotation/torque of a drive roller realized typically, by a dc servo-motor. The peripheral motion is transmitted to a bar (of appropriate matching surface form/profile) held against the drive-roller by a force transmitted through a 'squeeze' roller with its axis parallel to that of the drive-roller but on the opposite side of the bar. The squeeze 'preload' is typically generated by the deflection of coil-springs or a built-in flexure mechanism.

One variant employs a rectangular section bar and cylindrical rollers as shown in Figure 1.

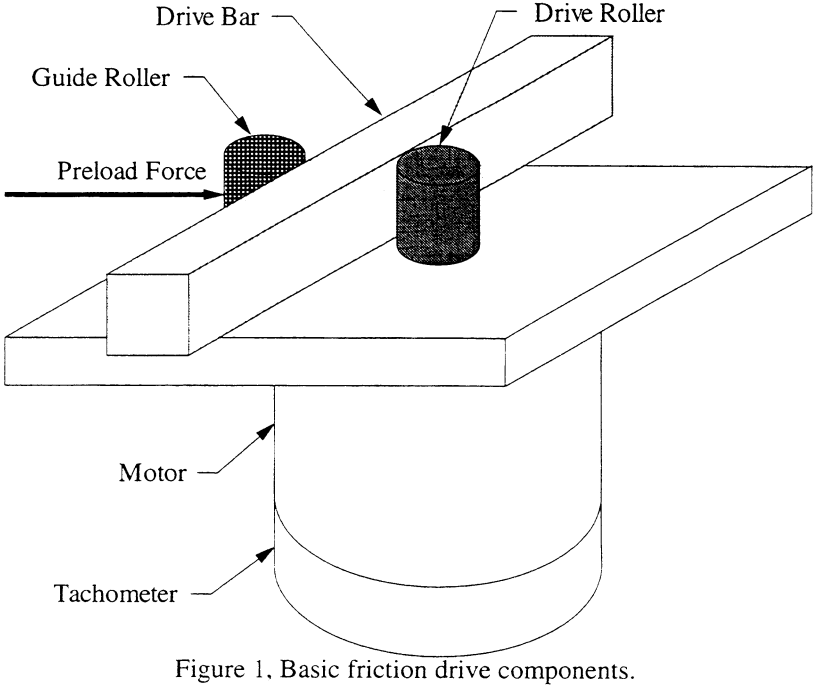

Figure 1, Basic friction drive components.

Another arrangement employs a cylindrical drive bar and V-shaped section drive and squeeze rollers, as shown in Figure 2. This provides increasing force against any tendency to 'steer off' and resultant self-aligning capability.

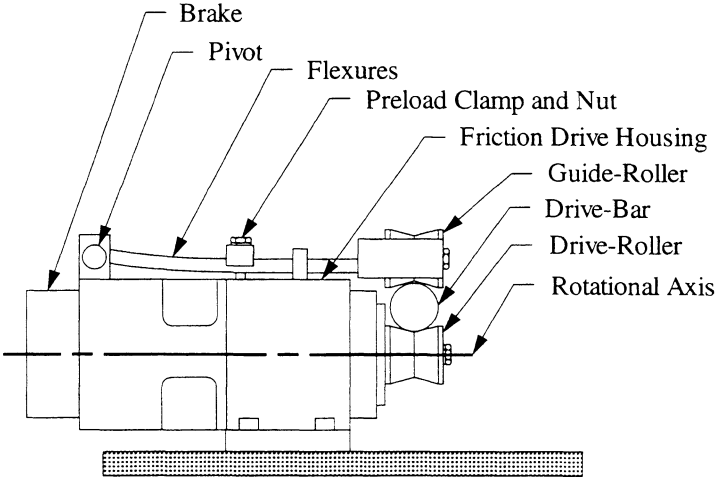

Side View
Figure 2, Side view of friction drive.

4 PROPERTIES AND FEATURES OF FRICTION-DRIVES

In working principle, friction/capstan traction-drives have many features in common with the rack-and-pinion drives. Positive features include:

- direct-mounting of drive unit onto moving carriage (eliminating couplings);
- low backlash and deadband control non-linearities (resulting from direct-mounting);
- low drive friction;
- low complexity in design;
- gearing readily specified within limits set by roller/bar geometries.

Less desirable features include:

- slippage at/between drive-roller/bar interface (i.e. drive force/torque limits);
- stiffness and damping limits due to material and geometrical properties of rollers/bar;
- transmission-gain (gearing) intrinsically low where roller/bar geometries match;
- sensitivity to particle ingress at interface (requiring extensible bellows etc.).

5 SLIPPAGE MECHANICS

The relationship between drive roller radius **R**, angular velocity ω and rectilinear velocity **V** is given by

$$\mathbf{V} = \mathbf{R}\omega \qquad (1)$$

At the limit of slippage, the axial drive force $\mathbf{F_d}$ is related to the torque τ by

$$\mathbf{F_d} = \tau/\mathbf{R} \qquad \mathbf{(2)}$$

If the coefficient of friction is μ, the relationship between the drive force $\mathbf{F_d}$ and preload force $\mathbf{F_p}$ is

$$\mathbf{F_p} = \mathbf{F_d}/\mu \qquad (3)$$

and for a given mass **m** and limiting acceleration **a**,

$$\mathbf{F_p} = \mathbf{ma}/\mu \qquad (4)$$

This equation governs the preload design for a given coefficient of friction and selected mass and/or acceleration. For systems with a moving drive rod, its mass should be minimized commensurate with stiffness.

6 DESIGN EXTENSIBILITY

The capstan/friction drive has considerable design flexibility in terms of range for a given drive force. Once the squeeze and drive roller geometry and force have been chosen, the range is set essentially by the length of the driven bar. With respect of commencement with a drive with modest range with a view to extension, the design has much to offer compared with, for example, the leadscrew actuator for which designs are essentially constrained once the length of the screw has been chosen.

7 INTERFACE CONTACT ZONES

Figure 3, shows the ellipsoidal contact zone caused by point contact between the drive-roller and drive-bar.

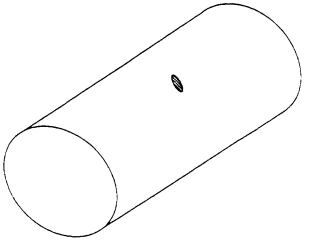

Figure 3, Elliptical contact zone between the drive-bar and one drive-roller surface.

The size of the ellipsoidal contact region and the maximum stress at the interface can be determined using the Hertz theory for contact between curved bodies.

The stresses caused by the contact between elastic bodies was developed by Hertz in 1881 (Seely and Smith, 1952) and has been solved for general cases by Roark (Young, 1989). The theory has been applied to rolling contact elements (Johnson, 1985) and has been used by many researchers to design and characterize friction drives, drive-rollers and drive-bars (Donaldson and Madux, 1984, Moronuki and Furukawa, 1988, Takahashi and Otsuka, 1989, Shimizu and Takeuchi 1990). The work for this paper is an extension of the theory to analyze the relative slip and the tangential stiffness (an axial stiffness located at the elliptical contact zone) at the surface of the contact interface for friction drives. Detailed analysis is presented in Slocum (1992) and Damazo (1995).

From this analysis, the relationship between tangential stiffness and applied load is very important to note. Figure 4, illustrates how stiffness

decreases when the tangential load applied increases. At low loads, the friction drive seems to provide a reasonably high stiffness (a stiffness higher than normally accredited); however, as the load approaches the maximum allowed by the preload force and coefficient of friction, stiffness begins to drop off more rapidly. This nonlinearity may affect the servo system stability if large inertial loads are allowed to occur during machine operation.

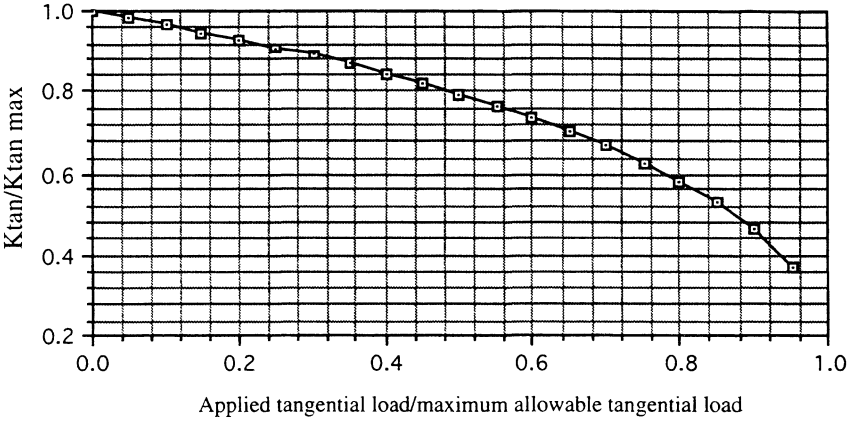

Figure 4, Theoretical effect of applied load on tangential stiffness for a friction drive.

8 STATIC STIFFNESS EXPERIMENTAL RESULTS

Static stiffness measurements were conducted. For each test, the bar was axially loaded with weights and then unloaded, while recording the drive-bar displacement at each weight increment. Straight lines are fitted to the data: the slopes represent the tangential stiffness. The straight lines are fitted using a linear regression of the displacement versus load data for both the load and the unload cases. The coefficient of friction was determined by taking the applied load that caused the drive-bar to then start to slip and dividing by the preload force.

Shown in Figure 5, are the measured static stiffness results for a 4300 N preload and no lubrication. For the loading condition, static stiffness is measured to be 101 N/μm. For the unloading condition, the static stiffness is measured to be 99 N/μm. The difference between the loading and the unloading conditions is perhaps representative of a tiny amount of slip or hysteresis present in the contact interface. The coefficient of friction for this case was measured to be 0.1. Table 1 summarizes the static stiffness results. Case one conditions represent no lubrication: a dry clean contact interface.

Table 1, Summary of Static Stiffness Results

Preload (N)	Case Conditions	Coefficient of Friction	Measured Tangential Stiffness (N/μm)
4300	one	0.1	101
3900	one	0.1	98
3500	one	0.1	92
3100	one	0.1	93

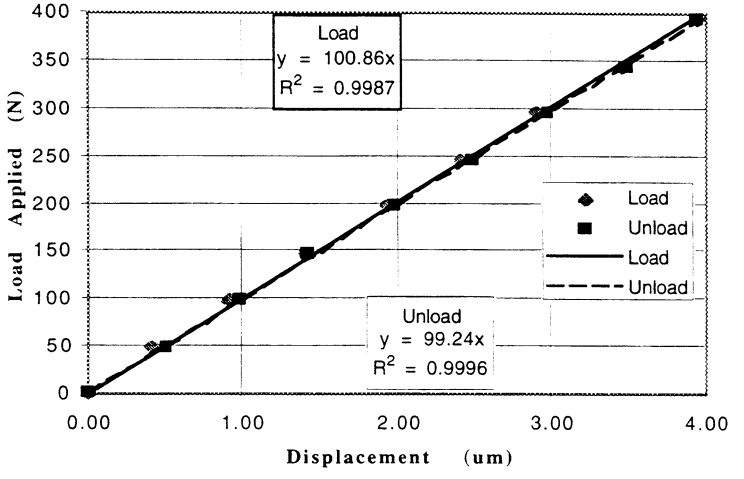

Figure 5, Static stiffness of the contact interface with no lubrication.

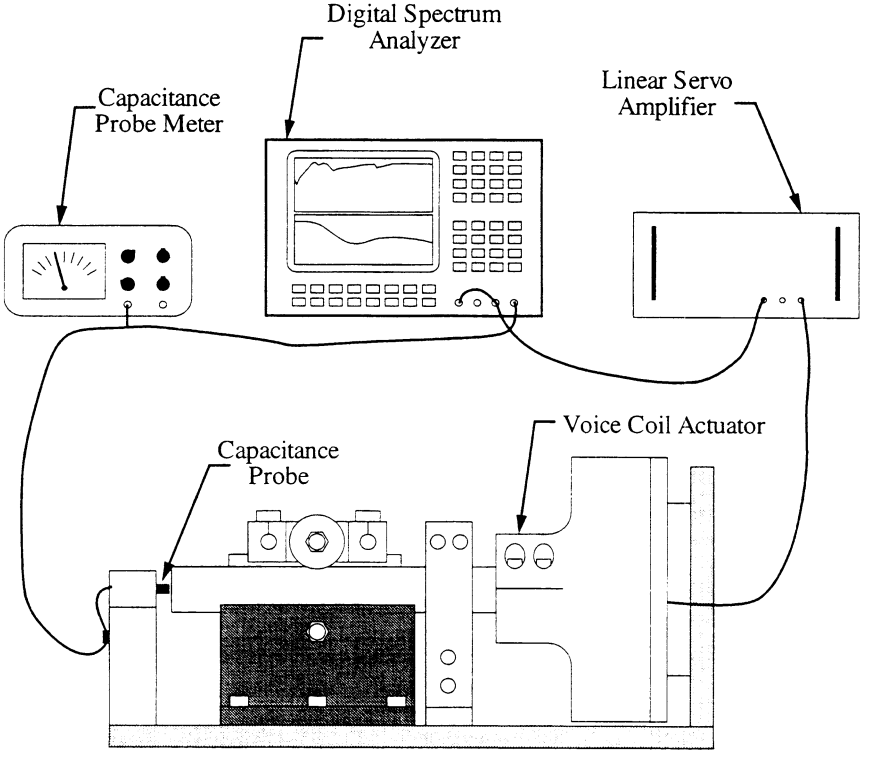

Figure 6, Friction drive test-stand configured with voice coil actuator (force input) and capacitance probe (displacement measurement) for the measurement of dynamic stiffness.

9 DYNAMIC STIFFNESS EXPERIMENTAL RESULTS

The dynamic stiffness of the contact interface was measured with the test-stand configuration as shown in Figure 6. The test-stand is configured with a electro-dynamic actuator (voice coil and magnet) assembly mounted to the drive-bar. This assembly is driven by a linear servo amplifier with a calibrated force/voltage constant. The signal to the servo amplifier is generated by a digital spectrum analyzer. The spectrum analyzer generates a sinusoidal voltage to drive the electro-dynamic actuator which produces a sinusoidal force on the contact interface. Displacement caused by the force input is measured with the capacitance probes, and is read by the digital spectrum analyzer. This measurement is a frequency response of the contact interface compliance (i.e. the inverse of the dynamic stiffness).

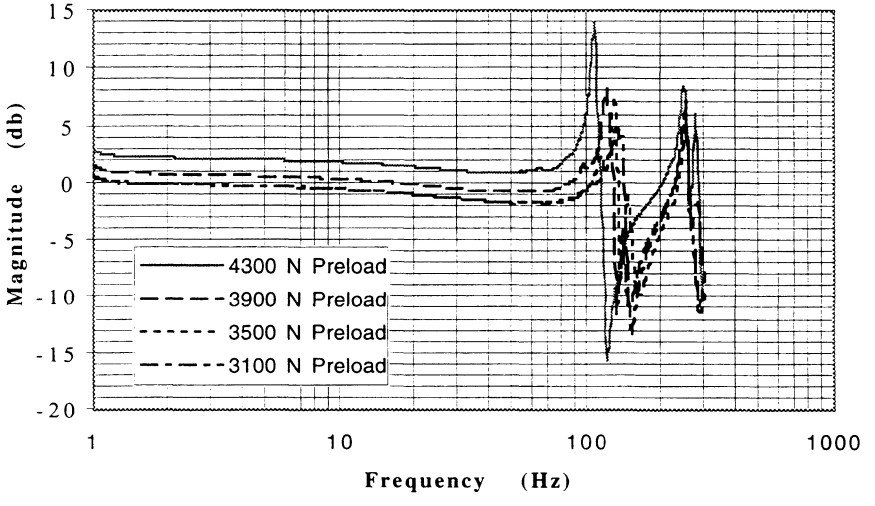

Figure 7, Frequency response of the contact interface dynamic compliance with no lubrication.

Table 2, Summary of contact interface dynamic stiffness results with no lubrication.

			Preload		
	Frequency (Hz)	4300 N	3900 N	3500 N	3100 N
Magnitude (db)	1	2.869	1.534	0.567	0.699
Stiffness (N/μm)	1	184	214	239	236
Magnitude (db)	50	1.003	-0.703	-1.67	-1.723
Stiffness (N/μm)	50	228	277	310	312

Shown in Figure 7 is the frequency response of the dynamic compliance for the no lubrication case with a summary in Table 2. When the preload was decreased, the measured stiffness actually increased as opposed to the theoretical values shown in Table 3. It was observed that the stiffness increased with the number of data sets collected, when the same contact interface points were used. When the drive-roller and drive-bar were rotated

to a new position, the stiffness decreased initially, then increased again with the number of data sets collected.

The variability in the results is suspected to be caused by asperities interlocking at the metal-to-metal contact interface. This interlocking would be facilitated by the sinusoidal force from the electro-dynamic actuator, applied to the drive bar. The measured dynamic stiffness is more than twice that measured for the static stiffness. This is due to the effect on the stiffness as a function of the applied tangential load shown in Figure 4.

Table 3, Comparison of measured dynamic stiffness at 1 Hz and theoretical tangential stiffness for no lubrication.

Preload (N)	Case Conditions	Maximum Applied Tangential Load (N)	Theoretical Tangential Stiffness (N/μm)	Measured Tangential Stiffness (N/μm)
4300	one	32	236	184
3900	one	32	228	214
3500	one	32	219	239
3100	one	32	210	236

10 CONCLUSIONS

This study provides an aide for the machine designer in selecting design parameters based on an extension of the well-established Hertzian contact theory. The result was a model to predict the compliant behavior of friction drives and the experimental results showed close correlation to this model. This enables the machine designer to compute friction drive (and resulting machine) performances and to ask 'what if' questions at the design stage before first building and testing a prototype. He/she should be able to save time and effort in the development of new generation machine tools and other high precision manufacturing systems.

REFERENCES

Chitayat A (1987) "Brushless DC Linear Motors" *Motion* vol 3, September/October pp 22-23.

Damazo, B N (1995) Ph. D Thesis, Cranfield University.

Donaldson, R., and Madux, A. (1984). "Design of a high-performance slide and drive system for a small precision machining research lathe," Ann CIRP, vol. 33, pp 1-14.

Gee A E (1982) " A 'Microincher' Machine Carriage Drive with Automatic Control of Step-pitch, Step-phase and Inter-step Positioning" *Prec Engg* vol 4 pp 85-92.

Harrison G R and Stroke G W (1955) "Interferometric Control of Grating Ruling with Continuous Carriage Advance" *J Opt Soc Am* vol 45 pp 112-121.

Harrison G R, Thompson S W, Kazukonis H and Connell J (1972) "750-mm Ruling Engine Producing Large Gratings and Echelles" *J Opt Soc Am* vol 62 pp 751-756.

Johnson, K. L. (1985). *Contact Mechanics*, Cambridge University Press, Cambridge United Kingdom.

May-Miller R (1985) "High Resolution Servo-positioning of a 370 kg Carriage" *3rd Intl Precision Engg Seminar*, Interlaken, Switzerland; abstracts pp 34-40 (Cranfield: CUPE and Zurich, Switzerland: ETH-IWF).

McKeown P A (1986) "High Precision and the British Economy" *Proc I Mech E* vol 200 pp 1-19.

Michelson A A (1915) "The Ruling and Performance of a Ten Inch Diffraction Grating" *Proc Am Phil Soc* vol 54 pp 137-142.

Moore W R (1970) *Foundations of Mechanical Accuracy* (Bridgeport CT: Moore Special Tool).

Moronuki, N., and Furukawa, Y. (1988). "On the design of precise feed mechanism by friction drive," *JSPE,* vol. 54, pp 81-85.

Sakuta, S. (1990). Toshiba Corp., commercial literature, Manufacturing Engineering Laboratory, 8 Shinsugita, Isogo, Yokohama, Kanagawa 235, Japan.

Seely, F. and Smith, J. (1952). *Advanced Mechanics of Materials*, John Wiley, New York.

Shimizu, H. and Takeuchi, Y. (1990). "Development of precision feed mechanism by means of friction drive," Proc. of Twenty-Eighth International Matador Conference, Manufacturing and Machine Tools Division, Dept. of Mechanical Engineering, UMIST Manchester, pp 527-532.

Slocum A (1992) *Precision Machine Design* (Englewood Cliffs NJ: Prentice-Hall).

Takahashi M and Otsuka J (1989) "Study on precision positioning by friction drive" *Proc. Int. Conf. on Advanced Mechatronics*, Tokyo, Japan, pp. 511-516.

Taniguchi N (1983) "Current Status in and Future Trends of Ultra-high Precision Machining and Ultra-Fine Materials Processing" Ann CIRP vol 32

Young, W. C., (1989). *Roark's Formulas for Stress and Strain*, 6th ed. McGraw-Hill, New York, pp 647-652.